Water transport through epoxy-based powder pipeline coatings

Hossein Zargarnezhad [a,*], Edouard Asselin [a] , Dennis Wong [b], C.N. Catherine Lam [b]

[a] *The University of British Columbia, Department of Materials Engineering, Department of Materials Engineering, 309-6350 Stores Road, Vancouver, BC V6T 1Z4, Canada*

[b] *Shawcor Ltd., 25 Bethridge Road, Toronto, ON, M9W 1M7, Canada*

** Corresponding author: hossein.zargar@ubc.ca (H. Zargarnezhad)*

ABSTRACT

Hydration of epoxy coatings reduces adhesion performance and causes degradation of the material, such as microstructural failures. Quantification of water vapor transport at elevated temperatures is fundamental to understanding polymer coating performance, especially when the coating is exposed to extreme operating conditions. As the water activity increases, the permeability/selectivity of polymers against other permeants changes. In this study, we examined the water permeation kinetics of two common epoxy-based powder coating systems for pipelines (fusion-bonded epoxy, FBE, and high-performance powder coating, HPPC) across a range of industrially-relevant temperatures (from room temperature to 80°C). Specifically, we utilized vapor permeation features of FBE and HPPC films with quantification of equilibrium flux as a function of temperature and pressure. In addition, we analyzed the nonlinear dependency of water transport on the vapor concentration at 65°C. The vapor transport analysis demonstrated that although data for FBE were indicative of a decrease in permeability around 65°C, perhaps due to self-association of water molecules,

the coating was likely to experience a plasticization pressure around this temperature. We also examined microstructural changes of the epoxy network due to water transport. Our results revealed evidence of irreversible damage to epoxy coatings under wet-state conditions above 65°C. It appears that the combination of thermal exposure and internal stresses in the glassy epoxy lead to a phase separation of filler particles from the epoxy matrix, as well as to a distinctive cavity formation in the coating membrane. Yet, despite formation of percolating paths for water transport, our results indicate that vapor permeation is primarily restrained due to self-association of water molecules. The vapor transport flux and its permeance are lowered by one order of magnitude in the multilayered HPPC thanks to the moisture-resistant polyethylene topcoat, thus reducing the extent of damage to the underlying substrate. Since barrier protection against gas phase diffusion is controlled by the FBE primer, however, consequences of coating hydration are more pronounced in the overall selectivity toward gaseous transport. Hydrothermal exposure is likely to increase aggregate porosity of the coating and a conservative implementation of standard coating requirements is therefore reasonable to avoid early degradation issues.

KEYWORDS

Fusion bonded epoxy, Vapor transport, Epoxy network, Polymer hydration, Water clustering.

1. Introduction

Water sorption and dynamic interactions between water and polymeric networks continue to attract scientific and technological interests to improve polymeric materials functionality and stability [1]–[4]. During water sorption and outgassing by polymeric coatings, the non-

equilibrium glassy state of the polymer, which prompts a gradual relaxation in polymeric chains, allows an additional uptake of water over time [5]. The resultant relaxation inevitably affects the barrier properties of the glassy polymer, as well as its resistance to degradation [6], [7]. In coating technologies, consequences of water uptake may affect adhesion strength, which is a central parameter in mitigation of undesired corrosion issues caused by mass transport across the protective coating [8]. Despite being primary components for pipeline coatings due to their good adhesion performance, epoxy materials are susceptible to moisture-induced degradation in wet environments [9], [10]. To provide a near-ideal protection against hydration, hydrophobic polymer structures are commonly added to the coating system as exterior layers [11], [12]. Yet, we do not fully understand failures that are witnessed on either single or multi-layer coatings [13], [14].

Although water absorption into a polymeric coating may not be the rate-determining step in the degradation process, it can gradually change the molecular structure of the polymeric coating and affect transmission of other species [5], [15]. Analysis of transport processes and their effects on degradation of pipeline coatings is scarce in the literature (see [16]) and studies linked with coatings' performances are usually focused on the disbonded areas upon local failures [17], [18]. Consequences of exposure to environmental parameters such as humidity, service temperature, pressure, and ageing can affect the coating performance [19]. In a recent extensive survey [18], we discussed the existing literature on wet-state diffusion systems and showed that mass transport rates of aggressive species surrounding an operating pipeline—such as gaseous and ionic permeants—may remarkably change due to polymer hydration. Fusion-bonded epoxy (FBE) is an example of a polymeric coating that is highly interactive with water. Based on reports for similar epoxy materials [5], [20], FBE is

likely to be highly permeable against moisture, but its permeability to oxygen is likely to be low — approximately 1.7×10^{-16} mol/m-s-Pa [21] compared to 7.1×10^{-16} mol/m-s-Pa for high-density polyethylene at 65°C [22]. FBE is also noted for purported qualities such as good adhesion and superior resistance to cathodic disbondment [23]. On the other hand, FBE has low impact resistance and a tendency to disbond from the steel substrate upon exposure to water at high temperatures (e.g., 65°C) [24]. High performance powder coating (HPPC) is another powder-based technology that enables a smooth transition from the glassy FBE to the compliant polyethylene (PE) topcoat while enhancing the overall resistance against moisture and mechanical damage [25]. HPPC showed excellent performance compared to conventional multilayering approaches by providing more uniform coverage, less residual stress, and less interlayer adhesion failure [25], [26]; however, since water interacts with the FBE primer, gradual hydration is anticipated and the multi-layered coating might be subjected to degradation of the FBE layer in long-term exposures to wet environments.

Water uptake and diffusion through epoxy coatings have been widely investigated in the literature, primarily to improve material properties during hygrothermal ageing [5], [27], [28]. The tendency of existing polar groups toward hydration can lead to nonlinearities in the vapor transmission–concentration relationship in hydrophilic membranes [29], [30]. A substantial increase in flux stems from a change in sorption process upon hygrothermal exposures; increasing hydration causes irreversible microdamage in the polymer network, which increase the amount of ‘trapped’ water in the pre-existing free volume (i.e., Langmuir type sorption) [5]. Loading polymers with additive fillers is a practical approach to enhance permeation performance of the resultant membrane by adjusting pore size and distribution [31], [32]. Layered silicate has been shown to reduce water absorption in epoxy resins,

although the silicate itself is neutral to the diffusion coefficient of water [33]. Based on prior results regarding the effects of additives on vapor transport [34], we could suggest that there may not be a direct relationship between filler particles and water sorption modes such as clustering. Yet, it seems that hydrophilic fillers pull out from the polymeric matrix in wet conditions [35]. Such an effect has been observed on the surface microstructure of FBE films after seven months of ageing at 85°C [14]. Yet, little empirical evidence exists to relate cross-sectional morphological changes to water permeation in epoxy coatings.

The objective of the following study was to characterize vapor transport through epoxy-based powder coating films. We carried out water vapor transmission (WVT) tests to directly assess water permeability through free coating films. We also analyzed water vapor permeability according to the activity of water (vapor pressure) for the critical temperature of 65°C to investigate permeation on the threshold of the coating plasticization. In addition, we investigated the extent of hydrothermal damage to the microstructure of the coating across a range of industrially-relevant test temperatures (25–80°C). Since water is expected to disrupt functional groups in the epoxy over time [24] and to affect microstructure of the coating throughout its transport, we also performed a qualitative analysis of the FBE microstructure after exposure to wet environments.

2. Experiments and methods

2.1. Materials and characterization

Various free-standing membranes with no intentional defects were investigated in this research. The water permeability of polymeric films was measured using a gravimetric cup

method [36]. Free films of all the coating materials, including FBE, topcoat PE, and HPPC, were supplied by Shawcor Ltd. The FBE used in this study has a glass transition temperature (T_g) of 110°C [37]. The coating membranes were cut individually into a circular plate, with a diameter of 7 cm. Each sample was measured for thickness using the geometric test area with an ultrasonic thickness gauge (Phase-II PTG-3750) that has an accuracy of 2 µm, and results are presented as means ± standard deviation.

For the analysis of water ingress into FBE, we followed an experimental procedure illustrated in Figure 1 and examined the coating microstructure of samples after each exposure condition. To investigate the effects of temperature and stress on the epoxy microstructure in wet environments, four free film samples and four FBE-coated steel panels (also supplied by Shawcor Ltd.) were immersed in a deionized (DI) water bath at 65°C (a and b, respectively, in Figure 1). Free films (with 4 cm^2 -coated areas) and steel panel samples (with 15 cm^2 -coated areas) were aged for 30 and 90 days. Steel panels were then cross-sectioned using cutting fluids to prevent hydrolytic degradation during elevated temperature exposure and then prepared for microstructural study. Coating cross-sections before and after permeation and immersion tests were examined using a FEI Quanta 650 scanning electron microscope (SEM) in back-scattered electron (BSE) mode at an accelerating voltage between 10 and 25 kV and magnification of up to 1000×. In addition, energy dispersive analysis was performed to investigate the elemental composition of filler particles. This characterization was carried out on the cross-sectioned, mounted, and polished free film samples. Lastly, to gain better insight into the distribution of defects inside the coating films, without exposing them to water during wet polishing, free film samples were immersed in liquid nitrogen for about 20 s and then broken to prepare cross-sections for

micromorphology observations. For all SEM examinations, compressed clean air was used to remove debris from samples, and the prepared cross sections were sputter-coated with a thin gold-palladium layer to provide conductivity.

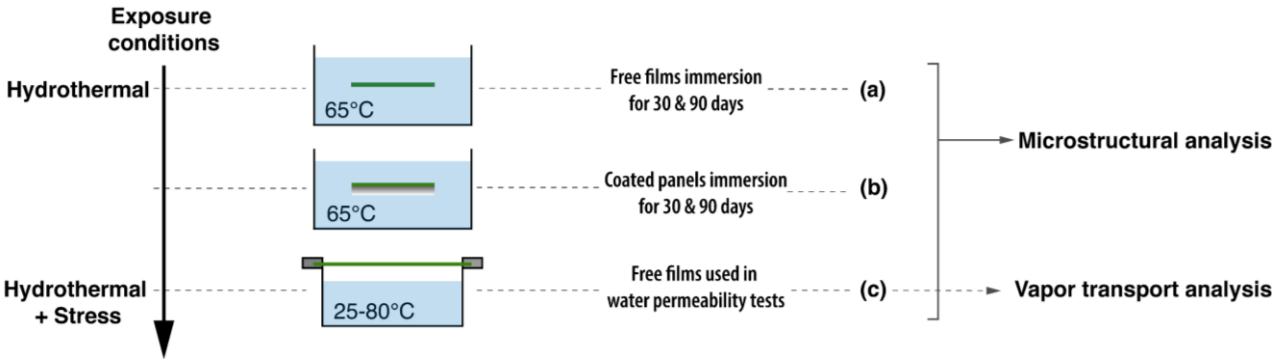

Figure 1. Schematic overview of the water ingress analysis for epoxy-based powder coatings

2.2. Water vapor permeability

To determine water permeability, we applied gravimetric cup methods based upon protocol ASTM D1653-03 (i.e., c in Figure 1) [36]. Vapometer cups, consisting of a container made of a noncorroding material impermeable to water, were used to measure the steady water vapor flow in unit time through unit area of a film under specific conditions of temperature and humidity at each face of the film. Exposure conditions were modified to measure vapor transmission above the standard temperatures. Dry cups contained fresh molecular sieve desiccant and wet-cups contained DI water to establish 0% and 100% relative humidity (RH), respectively, on one face of the coating sample. Each test specimen was sealed against the open mouth of a Vapometer cell (No. 68-3000, Thwing-Albert Instrument Co., West Berlin, NJ, USA) and the assembly was placed in the test chamber with a controlled atmosphere. The geometrical test area of the films was 31.67 cm^2, and the mass of the cup was

sequentially recorded over 12 days using an automated microbalance (with 1 mg sensitivity), allowing the effective permeability to be derived from the slope of the steady state mass change data over time. Test chamber temperatures were 25, 40, 65, 70, and 80°C and RH was generally maintained at 50%. For FBE films, tests at 65°C were piloted in several RH conditions (10, 30, and 50%) to investigate the effect of water activity on vapor transport. As per ASTM D1653, temperature and humidity inside the chamber were regulated at ± 1°C and ± 2%, respectively. Test conditions were also monitored externally with an EL-USB-2 temperature / humidity data logger (Lascar Electronics Ltd., PA, USA). Periodic weighing of cups was made in a few seconds to minimize errors due to internal pressure variations throughout each test and permeability data were taken as an average of three measurements (at minimum) for each test condition.

Based on the weight changes of each cup, we plotted the vapor transport flux against elapsed time. Vapor transmission rate or the normalized concentration-based permeability (P_L in mol/m-s) and gas phase permeability (P in mol/m-s-Pa) were calculated using:

$$P = \frac{P_L}{\Delta p} = \frac{J.l}{A(p_f - p_s)} \quad (1)$$

where J (mol/s) is the vapor flux resulting from the slope of the regression line, l (m) is the coating thickness, A (m^2) is the test area, p_f and p_s are absolute water pressure (Pa) on the vapor feed and vapor sink, respectively. Vapor pressures were derived from saturation pressure of water at the test temperature [38] times RH conditions (as decimals) at feed and sink sides.

2.3. Transport properties of the multilayered HPPC

HPPC is a composite membrane that has a configuration of a sealing (or protective) layer, a selective layer, and a support substrate which usually contains porosity – i.e., a polyethylene topcoat followed by a polyolefin adhesive and then an FBE primer [39], [40]. Vapor transmission through a defect-free laminate from different polymeric layers is expected to follow the ideal laminate theory [41]. Thus, WVT results for FBE and polyethylene topcoat samples are anticipated to yield a dependable estimate for P_L through an HPPC film – this assumes that the adhesive and topcoat layers are single PE layer. The permeability coefficient for a multilayer membrane (P^{HPPC}) is a function of the thickness (l^i) and permeability (P^i) of constituting layers, where:

$$\frac{P^{HPPC}}{\sum l^i} = \frac{1}{\sum l^i / P^i} \tag{2}$$

Validity of this equation for HPPC is typically studied at 65°C for WVT tests [5]. Due to unclear contribution of the constituting layers to the mass transfer resistance of the multilayered HPPC, we used permeance (mol/m^2-s-Pa) instead of permeability to assess the coating performance from direct empirical results, in which:

$$Permeance = \frac{J^{HPPC}}{A\Delta p} = \frac{P^{HPPC}}{\sum l^i} \tag{3}$$

where Δp is the pressure difference across the multilayered membrane as defined in Equation (1). Unlike permeability, the permeance is strongly dependent on the thickness of the membrane and driving force (e.g., upstream and downstream pressures); however, comparisons of permeance data are still expected to reflect variations in flux due to vapor-liquid equilibrium effects. In other words, although permeance can change with feed

pressure similar to flux, it does not do so as markedly, and analyses of transport based on permeance can provide insightful information [42].

3. Results and Discussion

3.1. Water transport analysis of FBE

We plotted vapor transport isotherms of FBE using a nonlinear regression analysis for different RH conditions at 65°C (Figure 2). Since data from dry- and wet-cup measurements were generated during exposure to lower and higher water vapor concentrations, respectively, higher absorption of water made the coating less dense, allowing moisture to transport at relatively higher rates [36]. At lower activities (e.g., measured data in dry-cup limits), water transmission rate increased with concentration close to a linear manner because the Langmuir and Henry's sorption modes, also known as dual-mode sorption, are dominant processes [43], [44]. We found a small nonlinear relationship between the water vapor transmission rate (i.e., P_L) and its concentration. The effect of water activity on transmission through FBE was also notable when the concentration gradient was high in either dry- or wet-cup isotherms. The non-linear trend suggests a transition in sorption or diffusion in the polymer network, which is often attributed to self-association of water inside the polymer [44], [45]. The hole-filling mechanisms (i.e., Langmuir and Henry's type sorption) reach an equilibrium above ~0.5 water activity, and a dynamic water clustering occurs in the glassy polymeric network—activation of pooling mode sorption [45]. That being said, the slight drifts from linearity for wet-cup limits in Figure 2 suggest the formation of less water clusters within FBE network as compared to other hygroscopic glassy polymers [46].

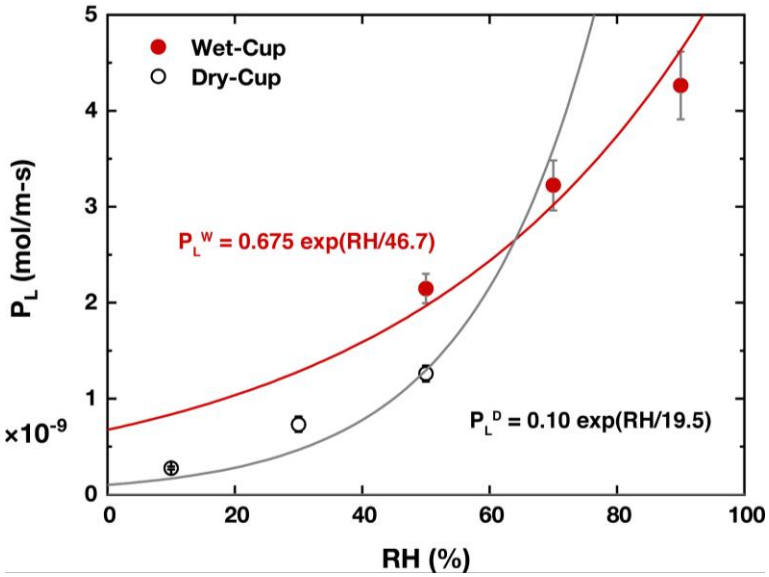

Figure 2. Vapor transmission results at 65ºC for vapometer cups with internal relative humidity of 0% and 100% (i.e., dry- and wet-cup limits, respectively) in external relative humidities of 10, 30, and 50%. Relative humidity inside the chamber was calculated as the ratio of the actual water vapor pressure to the saturated water vapor pressure of the air at the test temperature. Three replications were made for each test condition. Each data point is an average +/- standard deviation. Grey and red solid lines were obtained from extrapolation of P_L in dry- and wet-cup conditions (P_L^D and P_L^W, respectively).

Permeability analysis of the WVT data in Figure 2 showed little contrasts between permeabilities for each FBE isotherm – i.e., 10^{-13} and 1.8×10^{-13} mol/m-s-Pa on average from dry- and wet-cup measurements, respectively (Figure 3). The small difference between data within each humidity limit is rooted in approximation of the steady-state flow across films according to boundary conditions. Indeed, these values represent the average permeability associated with the dry- and wet-cup limits [47]. Previous work [48] has shown that these average permeabilities can be applied as baselines for constructing spot permeability curves

(solid line curves in Figure 3). Each curve generates two equal areas within its designated limits (triangular areas in Figure 3). The resultant area between the two curves provides valid approximates for average permeability in general cases outside the tested limits. For instance, when an *a priori* dry FBE coated steel pipe is in service at 65°C with an average RH value of 70%, one can use reference equations for P_D and P_W to estimate a range for the nominal permeability value within 0 and 70% RH – i.e., by finding a range in which equal areas are generated between the dry (and wet) curve and these RH limits.

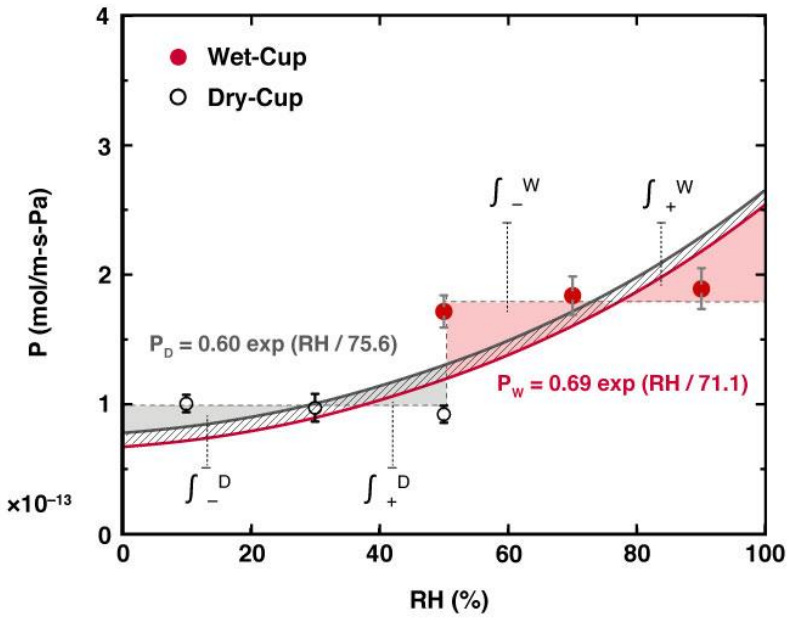

Figure 3. Average permeability data at 65ºC versus relative humidity and derivation of spot permeability curves for vapor transport. Each data point is an average +/- standard deviation. The spot permeability curves were obtained using a Brute-force integration over the two cup method results ($\left|\int_{-}^{D} - \int_{+}^{D}\right| / \int_{-}^{D} > 2 \times 10^{-8}$ & $\left|\int_{-}^{W} - \int_{+}^{W}\right| / \int_{-}^{W} > 7.5 \times 10^{-8}$).

Our results showed approximately one order of magnitude less permeability for water vapor than that reported previously by Fu and Cheng [49] − e.g., their analysis shows P_{FBE} = 18×10^{-13} mol/m-s-Pa for a wet-cup measurement at 65°C while it was 2×10^{-13} mol/m-s-Pa at similar conditions in this work. This may be due to different FBE formulations, or it may reflect these authors applying an imperfect sealing system in their cup method (i.e., using "water-proof epoxy resin" as a sealant). The data presented herein are in good agreement with results published in other literature for epoxy materials [5], [50]. Our study indicates that although measuring water vapor transmission rate and permeability at high temperatures can significantly vary with water activity, cup methods, if carefully implemented, can generate data with excellent confidence. Also, our quantification of water permeability versus vapor activity (i.e., spot permeability curves in Figure 3) can be used as a basis for modeling permeability parameters for FBE (i.e., the infinite dilution diffusivity, immobilization factor, and plasticization potential) in future studies [51].

The effect of thermal conditions on water transport also showed a nonlinear increase of vapor transmission rates as a function of temperature, ending with a significant rise (Figure 4). The final increase in P_L indicates that plasticization of the FBE occurs once the critical concentration of water within epoxy is exceeded during the temperature elevation, in other words when plasticization pressure is well below the vapor saturation pressure at 80°C. The difference between wet- and dry-cup results reached up to one order of magnitude at the upper limit, showing the extreme effect of vapor feed pressure on the transport process. Such a distinction at one test temperature also confirms that, at lower activities (dry-cup limits), water molecules are bonded at polar sites in the epoxy network and have less tendency for outgassing from the polymeric membrane. Previous work also showed that

translational and rotational movements of water molecules within the epoxy are hindered by the glassy and stiff structure at low concentrations [52]. According to Flory-Huggins theory [53]–[55], the interaction between a solvent (e.g., water) and a polymer is temperature dependent. This correlation helps explain why a narrow, almost negligible, margin exists between results from dry- and wet-cup tests at low temperatures (25 and 40°C in Figure 4). One must note that conditioning of the glassy polymer at these low temperatures enables the bonded water molecules to act as a nucleus for cluster formations [52]. By increasing temperature, the endothermic microvoid formation (or clustering) develops in the sorption process, and the associated irreversible process initiates microdamaging and degradation of the epoxy network [39].

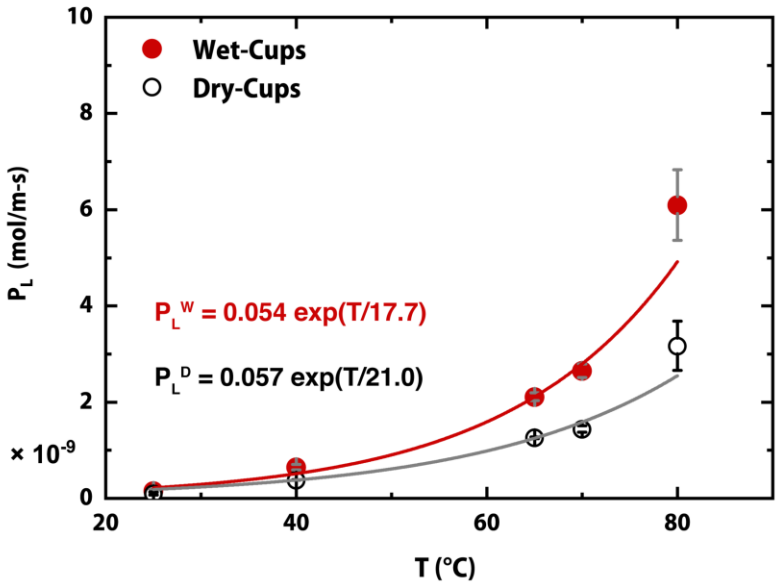

Figure 4. Water vapor transmission through fusion-bonded epoxy samples vs. temperature. Each data point is an average +/- standard deviation. Grey and red solid lines were obtained from extrapolation of P_L in dry- and wet-cup conditions (P_L^D and P_L^W, respectively); curves represent exponential regression analysis with probability values less than 0.005.

In general, gas phase permeability is an insubstantial function of concentration and temperature and does not follow an exponential growth similar to P_L [42]. In our study, changes in the average permeability of FBE at different temperatures, however, showed the synergistic effect of high temperature and pressure on vapor transport (Figure 5). Permeability initially increased as temperature was raised to 40°C, then followed a small declining trend in the middle range, but eventually turned up and began to increase due to plasticization effects. According to the van't Hoff-Arrhenius model, the temperature dependency of permeability through a polymer at a constant pressure is described by an energetic parameter and a pre-exponential factor (E_P and P_0 in $P = P_0 \exp(-E_P/RT)$, respectively [56]). This model predicts a progressive increase of permeability versus temperature in Figure 5. On the other hand, the pressure dependency of permeation through glassy polymers is a function of permeant/polymer interactions and one may encounter different qualitative trends by increasing feed pressure [57]. Generally, an initial decrease in permeability is followed by an increasing drift after a plasticization pressure, as described by the dual-mode sorption model [58], [59]. Accounting for the effect of temperature on the vapor pressure in Equation (1), the permeability data, as shown in Figure 5, are in agreement with previous findings on glassy polymers, which explain the gas permeability based on the predictions of the dual-mode sorption theory [58]. Additionally, the slight decrease of permeability between 40 and 65ºC in Figure 5 was also in accord with reports of water clustering effects in epoxy above 45°C, where the 'water-induced microvoid' situation became kinetically favorable due to its endothermic nature [52].

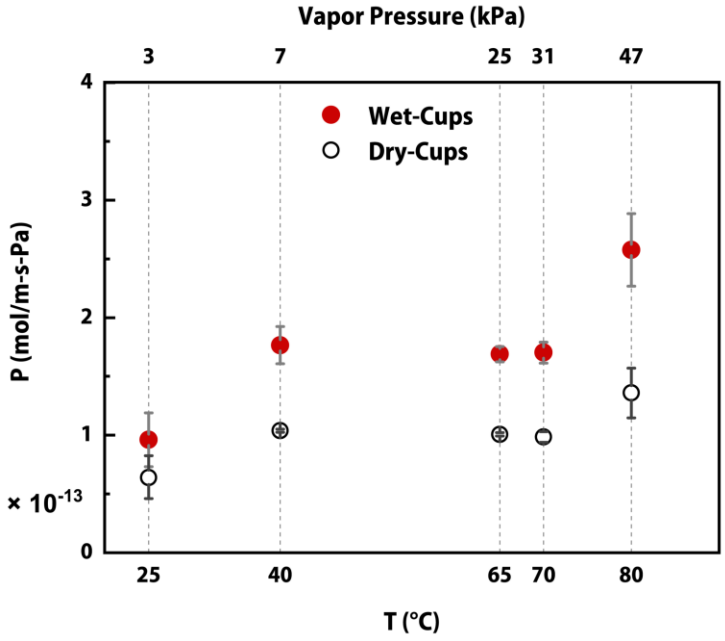

Figure 5. Water vapor permeability of fusion-bonded epoxy at different test temperatures. Each data point is an average +/- standard deviation.

Previous work [51] has shown through thermodynamic characterization of water clusters that formation of a more ordered structure from dissolved water has large enthalpy gain and entropy loss, resulting in a slightly negative ΔG. Specifically, the thermodynamically metastable state of water due to clustering slows the transmission rate through the polymeric network, resulting in a significant decrease of diffusivity of water molecules in the highly ordered water clusters. Upon further temperature increase (above 70°C) in our experimental design, the FBE network was plasticized by vapor permeant and concentration (or pressure) of the permeant became a determining factor in the barrier performance of the coating. In other words, although the clustering effect was likely to decrease permeability of the coating membrane, and therefore increase the selectivity over other permeants, the role of a permeant concentration is expected to become more pronounced for the hydrated polymer at elevated temperatures [50].

3.2. Microstructural degradation of FBE upon hydration

The cross-sectional morphologies of FBE film samples were examined by SEM; an example of a resulting image of an FBE coating is presented in Figure 6. With the energy dispersive X-ray analysis, we found acicular particles of calcium silicate dispersed within the FBE microstructure. The spectrum of the mapped area also indicated traces of magnesium and aluminum (below 7 and 2 mass %, respectively). Previous work has confirmed that the calcium silicate-rich fillers are needle-shape amorphous wollastonite ($CaSiO_3$), which is a functional filler added to increase flexural modulus and reduce the thermal expansion and shrinkage of the final coating [60]. Sugiman et al. demonstrated that adding micro-fillers into the epoxy resin decreases the crosslink density, subsequently increases the swelling strain during water transport [61]. On the other hand, increasing the volume fraction of fillers may subject the polymer to a percolation effect for water diffusion; a critical volume fraction (percolation threshold) of $p_c = 0.157$ is reported for epoxy composites [62]. For an average volume fraction of 0.074 ± 0.01 (0.037-0.12) inorganic content in the resin, with manufacturer specifications in parentheses, the FBE tested here would not be anticipated to experience a fast water uptake as a result of segregation of the absorbed water from the polymer chains [61]. High activities of water (> 0.8), however, have been shown to induce minor water clustering in epoxy systems similar to FBE [63]. If the filler is reactive with water, the time for reaching the saturation would increase, as diffusion rate would decrease, and water transport would be hindered due to the resulting trapping mechanism [35].

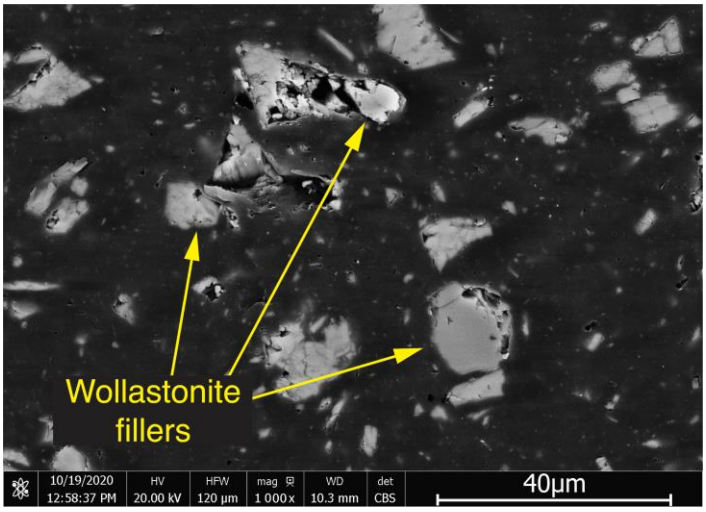

Figure 6. Back-scattered electron image of cross-sectional morphology of fusion-bonded epoxy microstructure; energy dispersive X-ray analysis of filler particles indicates presence of Ca and Si in high quantities (>45% and >40% atomic mass, respectively).

In our microstructural analysis, we observed pre-existing porosity defects in FBE coatings, and their size and distribution varied with the history and conditions of the coating application. According to the CSA Z245.20-18 standard released in 2018 [64], a coating is considered qualified if its associated porosity is lower than a certain limit; five rating scales are graphically defined for cross-section porosity and a coating should include equal to or less than that of rating three to be approved. Thus, unlike three-layer polyethylene systems in which no air entrapment is allowed in the topcoat layer [65], [66], the FBE coating may contain allowed cavities within its microstructure. The size and distribution of associated cavities are related to preheat temperature of the substrate, powder density of the spraying stream per pass applied and a possible minor contribution from evaporation of water/solvent compounds throughout the epoxy curing process [67].

We generated back-scattered electron (BSE) images from different water exposure conditions to show the extent of the damage of both immersion and WVT tests to the FBE films (Figure 7). Long-term exposure of FBE to 65°C DI water affected the interfacial bonds between epoxy resin and filler particles. As can be seen in Figure 7a, segregation of wollastonite particles from the epoxy-rich phase was distinct from unaged FBE (i.e., Figure 6). Upon addition of stress to the hydrothermal conditions (i.e., as in WVT films), shear deformation of the epoxy network was likely to occur, which would eventually cause microcracking and cavity formation (Figure 7b). It is pertinent to note that the morphology of the coating microstructure represented by the polished samples might yield an arbitrary representation of defects in the polymeric network. To further qualify the degradation, FBE free films were cryogenically sectioned and examined via SEM imaging (Figure 7c and d). When we compared the fracture surfaces of an unaged film sample and a film tested at a dry-cup assembly at 65°C, we found that coating degradation not only led to microcrack formations inside the epoxy, but it also resulted in less bonding between matrix and filler particles – wollastonite particles were highly incorporated in the epoxy resin in Figure 7c, whereas they were dispersed on the fracture surface in Figure 7d. It appears that hydrothermal exposure can cause excessive tearing and remarkably increase nonselective channels within the membrane. In a protective coating, such a deterioration can result in Knudsen flow (molecule-pore wall collisions) of penetrant molecules, and therefore poor barrier performance. The newly formed domains are taken up by water molecules in wet systems and associated clustering decreases the diffusivity (ergo the permeability) of permeants including water itself [68]. The polymeric coating, however, has already been subjected to severe damage and its barrier properties can significantly decline as soon as plasticization effects evolve at higher permeant temperatures or pressures [69].

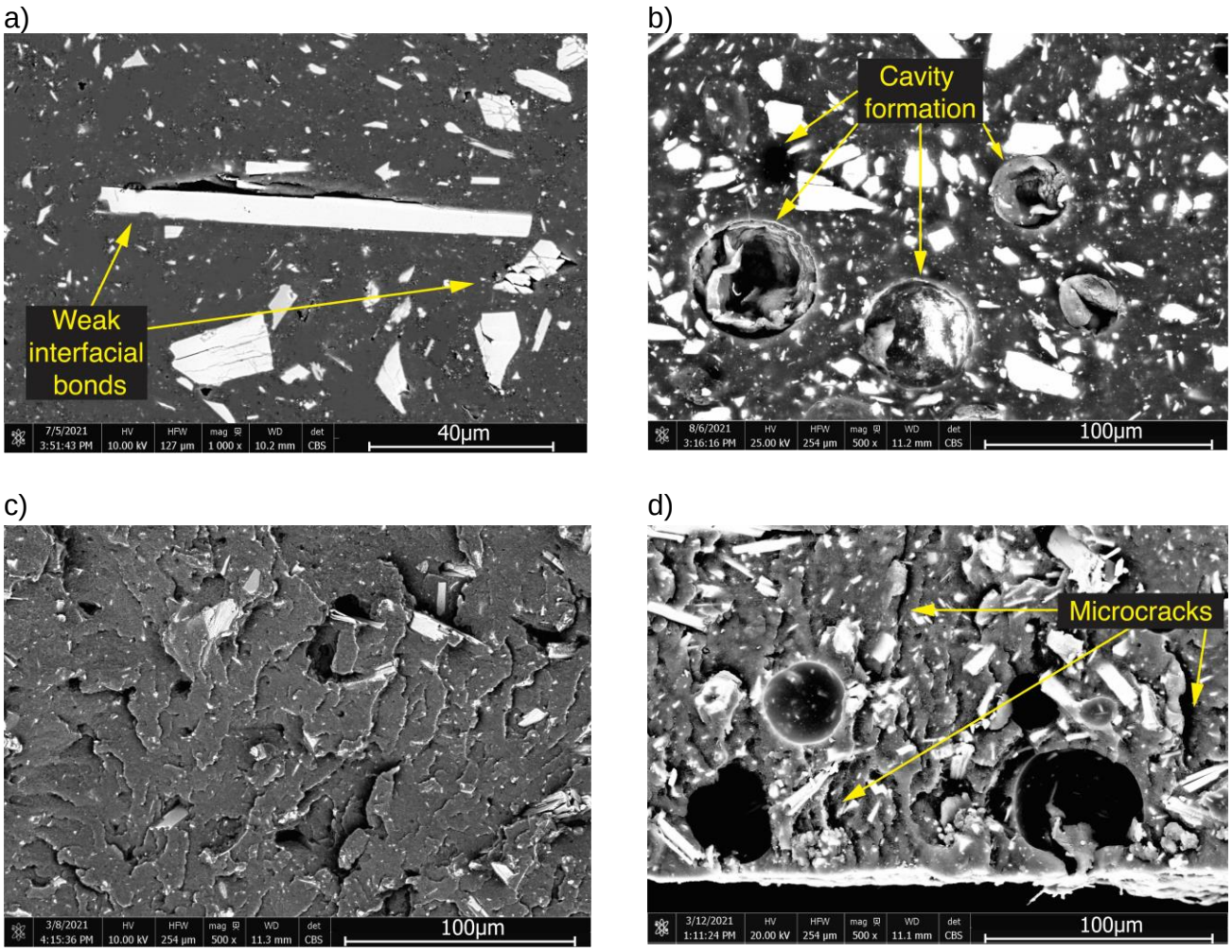

Figure 7. Micrographs of fusion-bonded epoxy: a) after exposure to 65°C deionized water for 90 days; b) after dry-cup water vapor transmission test at 65°C; c) cryogenic featuring of an unaged film; d) cryogenic featuring of film after dry-cup water vapor transmission test at 65°C.

According to both computational and experimental analyses of pipeline coatings, the energy associated with FBE that is applied on a steel substrate during manufacturing generates internal stresses inside the coating due to different thermal contraction coefficients between steel and thick (i.e., above 250 µm) polymeric coatings [24]. Comparative studies on epoxy-

free films and coatings during hygrothermal ageing confirm that diffusion kinetics increase with temperature (from 30°C to 60°C) and that diffusivity depends upon the microstructure (such as the polar group concentration and the free volume fraction) [46]. Although the polymer structure is locally modified in the applied coating and contains different diffusional pathways compared to free films, the relaxation of internal stresses in the applied coating during sorption is expected to decrease the diffusion rate close to the free film values [46]. Our SEM analysis indicated that the extent of polymer degradation in both free films and applied coatings was consistent and that long-term hydrothermal exposure to water at 65°C could lead to significant changes in porosity of applied FBE microstructure (Figure 8). We examined two different FBE panels for this analysis and compared the effect of hydrothermal exposure on specimens from these panels after 30 and 90 days. According to CSA Z245.20-18 [64], these panels were initially classified as rating of one and three (Figure 8a and c, respectively). After 30 days hydrothermal exposure, the coating microstructure was indicative of small cavity formations in the epoxy resin (Figure 8b compared to 8a). These micropore formations can induce further plasticization of the coating profile upon subsequent sorption of water. In other words, cross-section porosity present in the coating can increase during water permeation and, for instance, an unaged coating with the initial rating of three is highly likely to be classified as four or five after hydrothermal exposure (Figure 8c and d). Although clustering of absorbed molecules inside polymer reduces diffusional mobility inside epoxy upon formation of micropores, larger holes are expected to increase the solubility of the permeating water [21]. This degradation results in loss of selectivity of the coating, since transport behavior of the polymer can be highly dependent upon kinetics of water sorption/desorption processes within the polymer [5], [46]. In addition, appearance of interfacial disbondments of FBE was also notable in Figure 8d, which indicated that adhesion

loss and corrosion became thermodynamically favorable in the system (mass flux through coating correlates with transient occurrence of underlying corrosion reactions). This is of significance since immobilization of permeant at fixed sites within the polymeric medium, in microvoids or holes in the FBE structure, is highly temperature-dependent [34], and the gas held by these holes might be only partially immobilized [70].

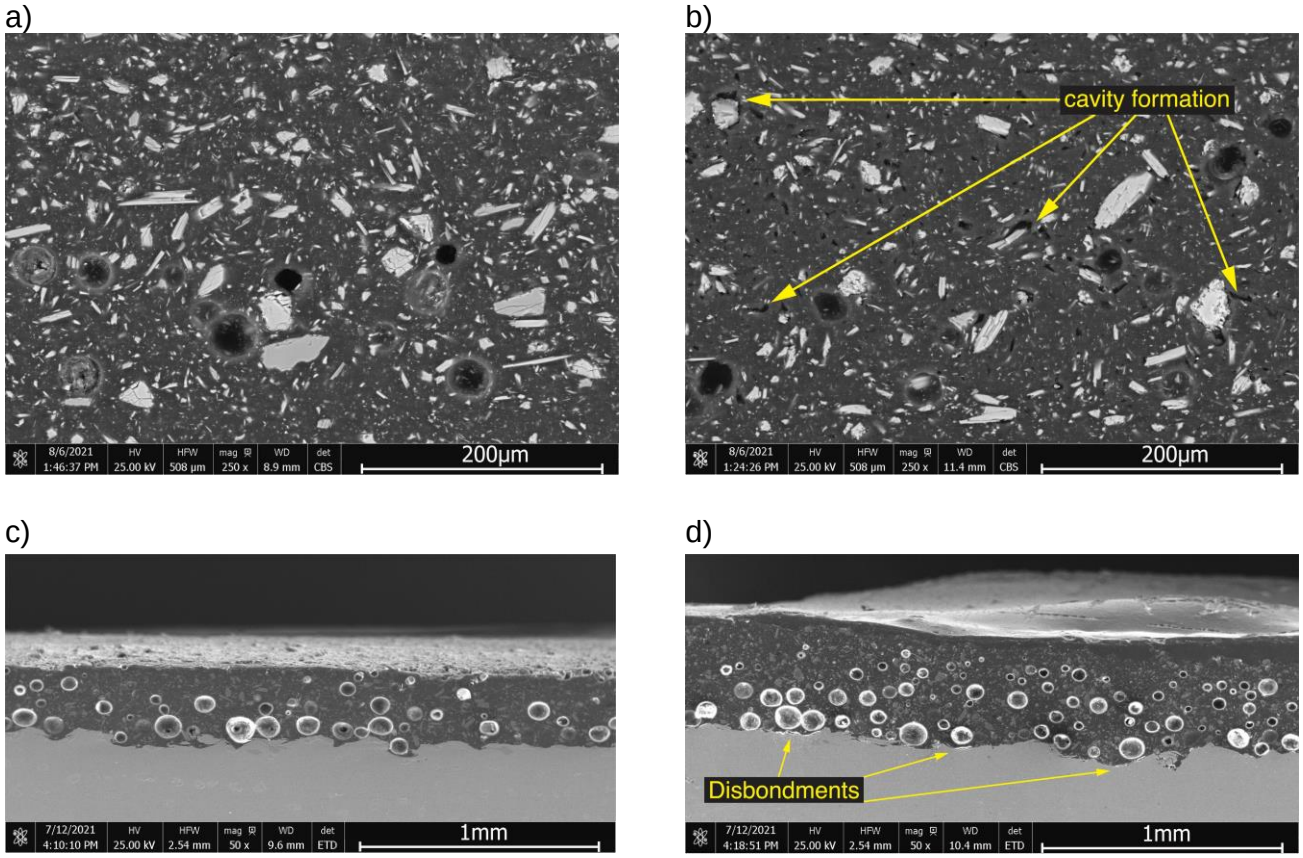

Figure 8. Micrographs of fusion-bonded epoxy panels: a) back-scattered electron image of an unaged specimen (rating of one); b) back-scattered electron image after immersion in 65°C deionized water for 30 days (initially classified as rating of one); c) secondary electron image of an unaged specimen (rating of three); d) secondary electron image after immersion

in 65°C deionized water for 90 days (initially classified as rating of three). CSA Z245.20-18 has been used as the classification criteria for the assessment of porosity in test specimens.

3.3. Vapor permeance through topcoat PE and HPPC

Vapor transmission rates through topcoat PE films at ambient temperatures (25 and 40°C) were outside the accuracy limit of the assembled WVT setup. For instance, a weight loss of ~0.04 mg/day is expected for a vapometer cell mounted with the topcoat PE sample at 25°C [62]. Therefore, for vapor transmission through topcoat PE and HPPC, the major focus was on measurements at elevated temperatures. Table 1 shows WVT results for topcoat PE films at different temperatures. As expected, both P_L and P increased linearly with temperature, and no significant contrast existed between data from different humidity limits, which conforms to anticipated properties of polyolefins.

Table 1. Permeability measurements for topcoat polyethylene

Test condition	Temperature	P_L* $(\times 10^{10})$	Permeance $(\times 10^{11})$	Permeability $(\times 10^{14})$
	°C	mol/m-s	mol/m^2-s-Pa	mol/m-s-Pa
Dry-cup	65	4.55 ±0.15	4.84 ±0.37	3.63 ±0.12
	70	6.49 ±1.05	5.52 ±1.04	4.16 ±0.96
	80	12.3 ±0.75	7.36 ±0.59	5.19 ±0.32
Wet-cup	65	4.66 ±0.41	4.82 ±0.52	3.72 ±0.33
	70	6.59 ±0.06	5.47 ±0.01	4.23 ±0.04
	80	13.3 ±1.06	7.75 ±0.60	5.62 ±0.45

* The normalized concentration-based permeability, as defined in Equation (1)

The projected permeance and experimental results for HPPC samples at 65°C are outlined in Table 2. Since permeance depends highly on the film thickness, and since contributions

of constituting layers in mass transport were not clear for HPPC (Figure 9), the application of ideal laminate theory (Equation 2) may not provide an effective assessment for mass transport analysis. Table 2 also shows that contrary to the results obtained from FBE, weight changes of dry-cup samples were slightly higher than that of wet-cup measurements for HPPC. This anomaly can be related to both the hygroscopicity of the FBE primer upon exposure to higher vapor concentrations and to the tendency of the primer for retaining moisture – in wet-cup measurements, this layer was exposed to 50% RH. Such moisture retention can cause a deviation from the established gradient across the HPPC film in wet-cup conditions. In contrast, in the dry-cup tests, moisture removal took place somewhat spontaneously, as the FBE primer was exposed to 0% RH. Although data from the lower RH range are more relevant for applied coatings, especially following application, wet-cup limit measurements can provide less conservative estimates for pipeline systems in equilibrium with their surrounding wet environments.

Table 2. Permeance data for high-performance powder coating

	Test condition	Temperature °C	Vapor flux $(\times 10^9)$ mol/s	Permeance $(\times 10^{11})$ mol/m^2-s-Pa
Data from Equation (2)	Dry-cup	65	–	3.92 ±0.20
	Wet-cup	65	–	4.28 ±0.28
Measurement data	Dry-cup	65	3.01 ±0.09	7.14 ±0.20
		70	4.16 ±0.50	7.93 ±0.95
		80	7.54 ±0.78	9.45 ±0.98
	Wet-cup	65	2.45 ±0.31	5.82 ±0.73
		70	3.15 ±0.04	6.00 ±0.06
		80	5.11 ±1.02	6.41 ±1.23

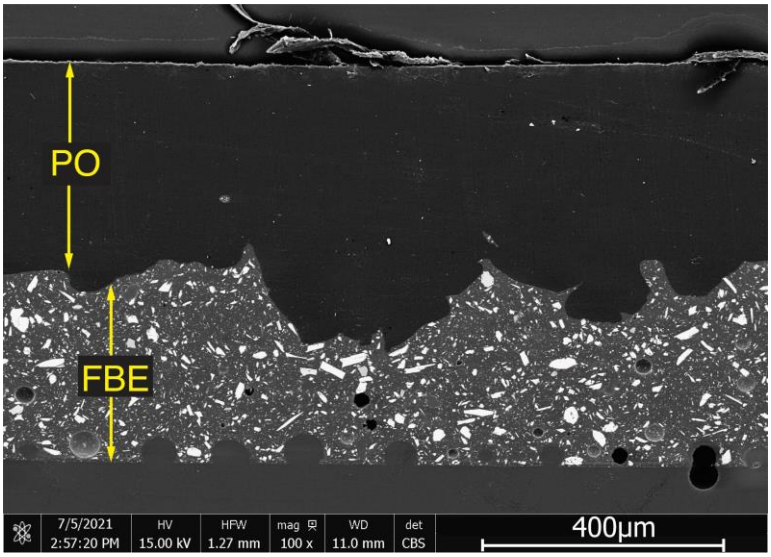

Figure 9. Back-scattered electron micrograph of cross-sectional morphology of high-performance powder coating. PO represents polyolefin adhesive + polyethylene topcoat.

As mentioned above, some of the previously reported data for epoxy coatings fail to accurately assess water permeability at elevated temperature conditions [11], [49]. This argument is further supported by comparing results for HPPC at 65°C, which showed around a two-order of magnitude higher permeance relative to our data (2.15×10^{-9} mol/m^2-s-Pa for HPPC in [49] compared to data for wet-cup measurement in Table 2). Interestingly, in an earlier work accomplished by the same research group as in [49], a significant vapor transmission rate was reported for the same membrane at room temperature (1.36×10^{-5} mol/m^2-s at 23°C in [11] compared to 5.4×10^{-5} mol/m^2-s at 65°C in [49] for HPPC under identical humidity conditions). This shows that misleading data may result from measurements on coating films unless a robust sealing system is used during measurements.

Since solubility of water molecules is the main driver of vapor permeability in the FBE structure [50], an additional moisture resistant layer can mitigate detrimental consequences

of interactions between water and the FBE. Results from Table 2 indicate that water vapor permeance can be reduced up to an order of magnitude via the multilayering approach. It should also be noted, however, that these data correspond to an upper boundary for the water transport; the coating and substrate adhesion forces mitigate water ingress prior to occurrence of a disbondment failure. On the other hand, such data provide the primary database to study selectivity of the coating membranes when permeation of other aggressive species (salt or gas) is likely. According to theories developed for gas separation and desalination membranes, the selectivity of a single layer membrane and the separation factor for a multilayered membrane are defined by the ratio of permeability and permeance, respectively, for multicomponent diffusion systems [40], [71]. Since water has a smaller kinetic diameter compared to other penetrants, it plays a key role in the barrier performance (i.e., selectivity or separation factor) of the coating. Thus, permeability data presented in this study enable quantitative analysis of the barrier performance of FBE and HPPC coatings [50].

4. Conclusion

Interactions between water and the epoxy network resulted in a nonlinear increase of vapor transmission rate versus concentration. At temperatures above 65°, the effect of water self-association became more pronounced in mass transport because water clusters can fill microvoids – either pre-existing or newly formed due to hydrothermal degradation. Once temperature exceeded 45°C and clustering of water molecules was kinetically favored, the water vapor permeability decreased slightly due to the reduction of diffusivity. At moderately high temperatures (i.e., above 70°C), however, the epoxy network became susceptible to

severe degradation and was plasticized once the threshold concentration was passed. Epoxy hydration at these temperatures would also diminish the interfacial adhesion between filler particles and epoxy resin. Under such conditions, if hydrothermal stress (either swelling pressure or internal stress) was added to the system, it could lead to microcracking and void formation in the coating membrane. The notion that hydrothermal exposure can alter the aggregate porosity of the coating may necessitate a careful review and implementation of industry standards for pipelines and other coated structures that are exposed to hydrothermal conditions.

In our study, multilayered HPPC was more resistant toward water ingress and shows transport behavior closer to topcoat PE. Due to the unknown contributions of its constitutive layers to overall permeability of this multilayered coating, the permeance parameter was a good reference to assess the membrane performance despite being heavily dependent on pressure and thickness. Empirical data and performance analyses presented in this study can shed light on barrier performance of the coatings of interest at elevated temperature. They can also provide a solid foundation to study selectivity performance of these materials in binary diffusion systems, such as wet gas permeation or salt ingress.

Acknowledgment

The authors acknowledge funding support from the Natural Sciences and Engineering Research Council (NSERC) of Canada [NSERC CRDPJ 503725-16]. The funding and in-kind support from Shawcor Ltd. and Specialty Polymer Coatings Inc. [Industry portion - NSERC CRDPJ 503725-16] are also greatly appreciated. The authors are also grateful to Mr. Parham Zarei for his valuable suggestions and kind collaboration for generating the brute force script for data analysis.

References

[1] S. J. Harley, E. A. Glascoe, and R. S. Maxwell, “Thermodynamic study on dynamic water vapor sorption in Sylgard-184,” *J. Phys. Chem. B*, vol. 116, pp. 14183–14190, 2012.

[2] S. J. Harley, E. A. Glascoe, J. P. Lewicki, and R. S. Maxwell, “Advances in modeling sorption and diffusion of moisture in porous reactive materials,” *ChemPhysChem*, vol. 15, pp. 1809–1820, 2014, doi: 10.1002/cphc.201301097.

[3] V. Baukh, H. P. Huinink, O. C. G. Adan, S. J. F. Erich, and L. G. J. Van Der Ven, “Water-polymer interaction during water uptake,” *Macromolecules*, vol. 44, pp. 4863–4871, 2011.

[4] Y. Liu, W. Soer, J. Scheerder, G. Satgurunathan, and J. L. Keddie, “Water vapor sorption and diffusion in secondary dispersion barrier coatings: A critical comparison with emulsion polymers,” *ACS Appl. Mater. interfaces*, vol. 7, pp. 12147–12157, 2015, doi: 10.1021/acsami.5b02446.

[5] E. Linde, N. H. Giron, and M. C. Celina, “Water diffusion with temperature enabling predictions for sorption and transport behavior in thermoset materials,” *Polymer (Guildf).*, vol. 153, pp. 653–667, 2018, doi: 10.1016/j.polymer.2018.08.024.

[6] P. Musto, G. Ragosta, and G. Mensitieri, “Time-resolved FTIR/FTNIR spectroscopy: Powerful tools to investigate diffusion processes in polymeric films and membranes,” *e-Polymers*, vol. 2, no. 1, 2002, doi: 10.1515/epoly.2002.2.1.220.

[7] M. Latino, F. Varela, Y. Tan, and M. Forsyth, “The effect of ageing on cathodic

protection shielding by fusion bonded epoxy coatings," *Prog. Org. Coatings*, vol. 134, pp. 58–65, 2019.

[8] R. J. Varley and K. H. Leong, "Polymer Coatings for Oilfield Pipelines," in *Active Protective Coatings: New-Generation Coatings for Metals*, A. E. Hughes, J. M. C. Mol, M. L. Zheludkevich, and R. G. Buchheit, Eds. Dordrecht, Netherlands: Springer, 2016, pp. 385–428.

[9] J. A. Kehr, *Fusion-bonded epoxy (FBE): a foundation for pipeline corrosion protection*. Houston, Texas, USA: NACE International, 2003.

[10] A. N. K. Jadoon and I. Thompson, "Fusion bonded epoxy mainline and field joint coatings performance from the X100 field trial - A case study," *Int. J. Press. Vessel. Pip.*, vol. 92, pp. 48–55, 2012, doi: 10.1016/j.ijpvp.2012.01.003.

[11] G. R. Howell and Y. F. Cheng, "Characterization of high performance composite coating for the northern pipeline application," *Prog. Org. Coatings*, vol. 60, no. 2, pp. 148–152, 2007, doi: 10.1016/j.porgcoat.2007.07.013.

[12] T. Byrnes, "Pipeline coatings," in *Trends in Oil and Gas Corrosion Research and Technologies*, Elsevier Ltd., 2017, pp. 563–591.

[13] M. Latino, F. Varela, M. Forsyth, and Y. Tan, "Self-validating electrochemical methodology for quantifying ionic currents through pipeline coatings," *Prog. Org. Coatings*, vol. 120, pp. 153–159, 2018, doi: 10.1016/j.porgcoat.2018.03.018.

[14] M. Latino, F. Varela, Y. Tan, and M. Forsyth, "The effect of ageing on cathodic protection shielding by fusion bonded epoxy coatings," *Prog. Org. Coatings*, vol. 134, no. April, pp. 58–65, 2019, doi: 10.1016/j.porgcoat.2019.04.074.

[15] J. Zhou and J. P. Lucas, "Hygrothermal effects of epoxy resin. Part I: the nature

of water in epoxy," *Polymer (Guildf).*, vol. 40, no. 20, pp. 5505–5512, 1999, doi: 10.1016/S0032-3861(98)00790-3.

[16] G. Bierwagen, D. Tallman, J. Li, L. He, and C. Jeffcoate, "EIS studies of coated metals in accelerated exposure," *Prog. Org. Coatings*, vol. 46, no. 2, pp. 149–158, 2003, doi: 10.1016/S0300-9440(02)00222-9.

[17] F. Mahdavi, M. Forsyth, and M. Y. J. Tan, "Techniques for testing and monitoring the cathodic disbondment of organic coatings: An overview of major obstacles and innovations," *Prog. Org. Coatings*, vol. 105, pp. 163–175, 2017, doi: 10.1016/j.porgcoat.2016.11.034.

[18] S. H. Lee, W. K. Oh, and J. G. Kim, "Acceleration and quantitative evaluation of degradation for corrosion protective coatings on buried pipeline: Part I. Development of electrochemical test methods," *Prog. Org. Coatings*, vol. 76, no. 4, pp. 778–783, 2013, doi: 10.1016/j.porgcoat.2012.06.010.

[19] A. Glaskova-Kuzmina, T. Aniskevich, G. Papanicolaou, D. Portan, A. Zotti, A. Borriello, and M. Zarrelli, "Hydrothermal aging of an epoxy resin filled with carbon nanofillers," *Polymers (Basel).*, vol. 12, no. 5, 2020, doi: 10.3390/POLYM12051153.

[20] M. K. Madhup, N. K. Shah, and N. R. Parekh, "Investigation and improvement of abrasion resistance, water vapor barrier and anticorrosion properties of mixed clay epoxy nanocomposite coating," *Prog. Org. Coatings*, vol. 102, pp. 186–193, 2017, doi: 10.1016/j.porgcoat.2016.10.012.

[21] M. C. Celina and A. Quintana, "Oxygen diffusivity and permeation through polymers at elevated temperature," *Polymer (Guildf).*, vol. 150, pp. 326–342,

2018, doi: 10.1016/j.polymer.2018.06.047.

[22] A. S. Michaels and H. J. Bixler, “Flow of gases through polyethylene,” *J. Polym. Sci.*, vol. 50, no. 154, pp. 413–439, 1961, doi: 10.1002/pol.1961.1205015412.

[23] M. Xu, C. N. C. Lam, D. Wong, and E. Asselin, “Evaluation of the cathodic disbondment resistance of pipeline coatings – A review,” *Prog. Org. Coatings*, vol. 146, p. 105728, 2020, doi: 10.1016/j.porgcoat.2020.105728.

[24] E. Legghe, E. Aragon, L. Bélec, A. Margaillan, and D. Melot, “Correlation between water diffusion and adhesion loss: Study of an epoxy primer on steel,” *Prog. Org. Coatings*, vol. 66, no. 3, pp. 276–280, 2009, doi: 10.1177/1942602X15619756.

[25] C. N. C. Lam, D. T. Wong, R. E. Steele, and S. J. Edmondson, “A new approach to high performance polyolefin coatings,” in *Corrosion Conference and Expo*, 2007, no. 07023.

[26] M. Xu, E. Asselin, C. Lam, and D. Wong, “Modified Cathodic Disbondment Test Methods for Comparing the Performance of HPPC and FBE Coatings,” *CORROSION 2021*. Apr. 2021.

[27] G. Z. Xiao, M. Delamar, and M. E. R. Shanahan, “Irreversible interactions between water and DGEBA / DDA epoxy resin during hygrothermal aging,” *J. Appl. Polym. Sci.*, vol. 65, no. 3, pp. 449–458, 1997.

[28] G. Z. Xiao and M. E. R. Shanahan, “Swelling of DGEBA/DDA epoxy resin during hygrothermal ageing,” *Polymer (Guildf).*, vol. 39, no. 14, pp. 3253–3260, 1998, doi: 10.1016/S0032-3861(97)10060-X.

[29] C. Mo, W. Yuan, W. Lei, and Y. Shijiu, “Effects of temperature and humidity on

the barrier properties of biaxially-oriented polypropylene and polyvinyl alcohol films," *J. Appl. Packag. Res.*, vol. 6, no. 1, pp. 40–46, 2014, doi: 10.14448/japr.01.0004.

[30] Z. Zhang, I. J. Britt, and M. A. Tung, "Permeation of oxygen and water vapor through EVOH films as influenced by relative humidity," *J. Appl. Polym. Sci.*, vol. 82, no. 8, pp. 1866–1872, 2001, doi: 10.1002/app.2030.

[31] S. Simone, A. Figoli, A. Criscuoli, M. C. Carnevale, A. Rosselli, and E. Drioli, "Preparation of hollow fibre membranes from PVDF/PVP blends and their application in VMD," *J. Memb. Sci.*, vol. 364, no. 1–2, pp. 219–232, 2010, doi: 10.1016/j.memsci.2010.08.013.

[32] J. Lee, B. Park, J. Kim, and S. Bin Park, "Effect of PVP, lithium chloride, and glycerol additives on PVDF dual-layer hollow fiber membranes fabricated using simultaneous spinning of TIPS and NIPS," *Macromol. Res.*, vol. 23, no. 3, pp. 291–299, 2015, doi: 10.1007/s13233-015-3037-x.

[33] O. Becker, R. J. Varley, and G. P. Simon, "Thermal stability and water uptake of high performance epoxy layered silicate nanocomposites," *Eur. Polym. J.*, vol. 40, no. 1, pp. 187–195, 2004, doi: 10.1016/j.eurpolymj.2003.09.008.

[34] G. K. Van Der Wel and O. C. G. Adan, "Moisture in organic coatings - a review," *Prog. Org. Coatings*, vol. 37, no. 1, pp. 1–14, 1999, doi: 10.1016/S0300-9440(99)00058-2.

[35] S. Sugiman and S. Salman, "Hygrothermal effects on tensile and fracture properties of epoxy filled with inorganic fillers having different reactivity to water," *J. Adhes. Sci. Technol.*, vol. 33, no. 7, pp. 691–714, 2019, doi:

10.1080/01694243.2018.1558492.

[36] ASTM D1653-03, “Standard Test Methods for Water Vapor Transmission of Organic Coating Films,” American Society for Testing Materials, West Conshohocken, PA, 2003.

[37] J. A. Kehr and D. G. Enos, “FBE, a foundation for pipeline corrosion coating,” in *Corrosion*, 2000, pp. 1–20.

[38] D. R. Lide, *CRC Handbook of Chemistry and Physics, 85th Edition*, 85th ed. CRC Press, 2004.

[39] T. S. Chung, J. J. Shieh, W. W. Y. Lau, M. P. Srinivasan, and D. R. Paul, “Fabrication of multi-layer composite hollow fiber membranes for gas separation,” *J. Memb. Sci.*, vol. 152, no. 2, pp. 211–225, 1999, doi: 10.1016/S0376-7388(98)00225-7.

[40] Z. Dai, L. Ansaloni, and L. Deng, “Recent advances in multi-layer composite polymeric membranes for CO2 separation: A review,” *Green Energy and Environment*, vol. 1, no. 2. Elsevier Ltd, pp. 102–128, 2016, doi: 10.1016/j.gee.2016.08.001.

[41] A. Grüniger and P. R. Von Rohr, “Influence of defects in SiOx thin films on their barrier properties,” *Thin Solid Films*, vol. 459, no. 1–2, pp. 308–312, 2004, doi: 10.1016/j.tsf.2003.12.146.

[42] R. W. Baker, J. G. Wijmans, and Y. Huang, “Permeability, permeance and selectivity: A preferred way of reporting pervaporation performance data,” *J. Memb. Sci.*, vol. 348, no. 1–2, pp. 346–352, 2010, doi: 10.1016/j.memsci.2009.11.022.

[43] H. N. Sharma, S. J. Harley, Y. Sun, and E. A. Glascoe, “Dynamic triple-mode sorption and outgassing in materials,” *Sci. Rep.*, vol. 7, no. 1, pp. 1–12, 2017, doi: 10.1038/s41598-017-03091-3.

[44] E. M. Davis and Y. A. Elabd, “Prediction of water solubility in glassy polymers using nonequilibrium thermodynamics,” *Ind. Eng. Chem. Res.*, vol. 52, pp. 12865–12875, 2013.

[45] E. M. Davis and Y. A. Elabd, “Water clustering in glassy polymers,” *J. Phys. Chem. B*, vol. 117, no. 36, pp. 10629–10640, 2013, doi: 10.1021/jp405388d.

[46] G. Bouvet, N. Dang, S. Cohendoz, X. Feaugas, S. Mallarino, and S. Touzain, “Impact of polar groups concentration and free volume on water sorption in model epoxy free films and coatings,” *Prog. Org. Coatings*, vol. 96, pp. 32–41, 2015, doi: 10.1016/j.porgcoat.2015.12.011.

[47] S. C. Chang and N. B. Hutcheon, “Dependence of water vapor permeability on temperature and humidity,” *Heating, Piping, Air Cond.*, no. 3, pp. 149–155, 1956.

[48] F. A. Joy and A. G. Wilson, “Standardization of the dish method for measuring water vapor transmission,” in *International Symposium on Humidity and Moisture, Proceedings*, 1963, pp. 259–270.

[49] A. Q. Fu and Y. F. Cheng, “Characterization of the permeability of a high performance composite coating to cathodic protection and its implications on pipeline integrity,” *Prog. Org. Coatings*, vol. 72, no. 3, pp. 423–428, 2011, doi: 10.1016/j.porgcoat.2011.05.015.

[50] H. Zargarnezhad, E. Asselin, D. Wong, and C. Lam, “A critical review of the time-dependent performance of polymeric pipeline coatings: Focus on hydration of

epoxy-based coatings," *Polymers (Basel).*, vol. 13, no. 9, p. 1517, 2021, doi: 10.3390/polym13091517.

[51] C. A. Scholes, J. Jin, G. W. Stevens, and S. E. Kentish, "Competitive permeation of gas and water vapour in high free volume polymeric membranes," *J. Polym. Sci. Part B Polym. Phys.*, vol. 53, no. 10, pp. 719–728, 2015, doi: 10.1002/polb.23689.

[52] C. Carfagna and A. Apicella, "Physical degradation by water clustering in epoxy resins," *J. Appl. Polym. Sci.*, vol. 28, pp. 2881–2885, 1983.

[53] P. J. Flory, *Principles of Polymer Chemistry*. London: Cornell University Press, 1953.

[54] P. J. Flory, "Thermodynamics of high polymer solutions," *J. Chem. Phys.*, vol. 9, no. 8, pp. 660–661, 1941, doi: 10.1063/1.1750971.

[55] M. L. Huggins, "Solutions of long chain compounds," *J. Chem. Phys.*, vol. 9, no. 5, p. 440, 1941, doi: 10.1063/1.1750930.

[56] S. Maghami, A. Mehrabani-zeinabad, M. Sadeghi, and J. Sánchez-laínez, "Mathematical modeling of temperature and pressure effects on permeability , diffusivity and solubility in polymeric and mixed matrix membranes," *Chem. Eng. Sci.*, vol. 205, pp. 58–73, 2019, doi: 10.1016/j.ces.2019.04.037.

[57] M. Minelli, S. Oradei, M. Fiorini, and G. C. Sarti, "CO2 plasticization effect on glassy polymeric membranes," *Polymer (Guildf).*, vol. 163, no. December 2018, pp. 29–35, 2019, doi: 10.1016/j.polymer.2018.12.043.

[58] A. F. Ismail and W. Lorna, "Penetrant-induced plasticization phenomenon in glassy polymers for gas separation membrane," *Sep. Purif. Technol.*, vol. 27, pp.

173–194, 2002.

[59] A. Bos, I. G. M. Punt, M. Wessling, and H. Strathmann, “CO2-induced plasticization phenomena in glassy polymers,” *J. Memb. Sci.*, vol. 155, pp. 67–78, 1999.

[60] P. A. Saliba, A. A. Mansur, D. B. Santos, and H. S. Mansur, “Fusion-bonded epoxy composite coatings on chemically functionalized API steel surfaces for potential deep-water petroleum exploration,” *Appl. Adhes. Sci.*, vol. 3, no. 1, 2015, doi: 10.1186/s40563-015-0052-2.

[61] S. Sugiman, S. Salman, and M. Maryudi, “Effects of volume fraction on water uptake and tensile properties of epoxy filled with inorganic fillers having different reactivity to water,” *Mater. Today Commun.*, vol. 24, no. June, 2020, doi: 10.1016/j.mtcomm.2020.101360.

[62] A. Lekatou, S. E. Faidi, D. Ghidaoui, S. B. Lyon, and R. C. Newman, “Effect of water and its activity on transport properties of glass/epoxy particulate composites,” *Compos. Part A Appl. Sci. Manuf.*, vol. 28, no. 3, pp. 223–236, 1997, doi: 10.1016/S1359-835X(96)00113-3.

[63] C. Vosgien Lacombre, G. Bouvet, D. Trinh, X. Feaugas, S. Touzain, and S. Mallarino, “Influence of pigment and internal stresses on water uptake in model epoxy: a thermodynamic approach,” *J. Mater. Sci.*, vol. 53, no. 3, pp. 2253–2267, 2018, doi: 10.1007/s10853-017-1647-8.

[64] CSA Z245.20-18, “Plant-applied external fusion bond epoxy coating for steel pipe,” 2018.

[65] A. Bahadori, “Chapter 8 - Materials and Construction for Three-Layer

Polyethylene Coating Systems," in *Essentials of Coating, Painting, and Lining for the Oil, Gas and Petrochemical Industries*, Elsevier Inc., 2015, pp. 473–498.

[66] DIN 30670, "Polyethylene coatings on steel pipes and fittings - Requirements and testing," 2012.

[67] C. Yi, P. Rostron, N. Vahdati, E. Gunister, and A. Alfantazi, "Curing kinetics and mechanical properties of epoxy based coatings: The influence of added solvent," *Prog. Org. Coatings*, vol. 124, no. May, pp. 165–174, 2018, doi: 10.1016/j.porgcoat.2018.08.009.

[68] A. D. Drozdov, J. Christiansen, R. K. Gupta, and A. P. Shah, "Model for Anomalous Moisture Diffusion through a Polymer – Clay Nanocomposite," *J. Polym. Sci. Part B Polym. Phys.*, vol. 41, pp. 476–492, 2003.

[69] D. F. Sanders *et al.*, "Energy-efficient polymeric gas separation membranes for a sustainable future: A review," *Polymer (Guildf).*, vol. 54, no. 18, pp. 4729–4761, 2013, doi: 10.1016/j.polymer.2013.05.075.

[70] D. R. Paul, W. J. Koros, and C. Engineering, "Effect of partially immobilizing sorption on permeability and the diffusion time lag," *J. Polym. Sci. Polym. Phys. Ed.*, vol. 14, pp. 675–685, 1976.

[71] B. D. Freeman, "Basis of permeability/selectivity tradeoff relations in polymeric gas separation membranes," *Macromolecules*, vol. 32, no. 2, pp. 375–380, 1999, doi: 10.1021/ma9814548.